Biophysical Journal

Supporting Material

Diffusion Regulation in the Vitreous Humor

Benjamin Tillmann Käsdorf,[1,2] Fabienna Arends,[1,2] and Oliver Lieleg[1,2,*]

[1]Institute of Medical Engineering (IMETUM) and [2]Department of Mechanical Engineering, Technische Universität München, Garching, Germany

Table T1: Estimated charge state of particles and molecules used. The maximal number of charged groups on polystyrene particles, liposomes, FITC-dextrans and TAMRA-peptides at physiological pH was estimated based on particle/molecule size, molecule structure, pK_a of the specific groups and supplier information.

	Particle type	**Particle size [nm]**	**Estimated max. net charge [e] at pH 7.3**
polystyrene particles	carboxyl	~ 200	~ 10^6 (-)
	PEG		~ 0 (assuming full PEGylation)
	amine		~ 10^6 (+)
liposomes	DOPG/Rh	~ 200	~ 10^5 (-)
	DOPC/DOTAP/Rh		~ 0
	DOTAP/Rh		~ 10^5 (-)
4 kDa *FITC-dextrans* 150 kDa	CM	~ 1.4	~ 5 (-)
	unmod.		~ 1 (-)
	DEAE		~ 5 (+)
	CM	~ 8.5	~ 160 (-)
	unmod.		~ 4 (-)
	DEAE		~ 200 (+)
TAMRA-peptides (~ 4 kDa)	P1 – $(EEE)_8$	~ 1.5	25 (-)
	P2 – $(QQE)_8$		9 (-)
	P3 – $(QQK)_8$		7 (+)
	P4 – $(QK)_{12}$		11 (+)
	P5 – $(QKK)_8$		15 (+)
	P6 – $(QKKKK)_4$		19 (+)
	P7 – $(KKK)_8$		23 (+)

Distribution of apparent diffusion coefficients for polystyrene particles and liposomes in mammalian vitreous humor.

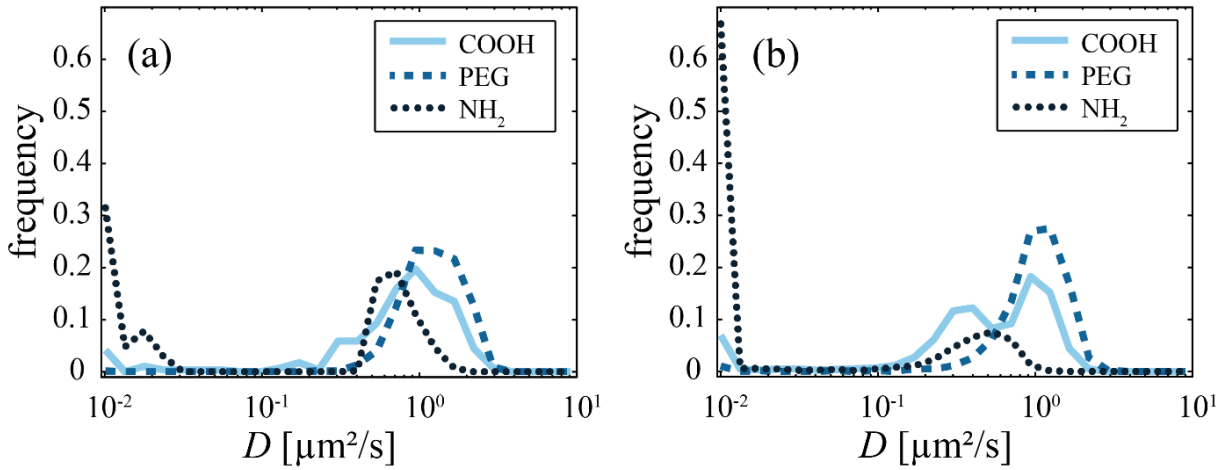

Fig. S1: Diffusive mobility of 200 nm polystyrene particles in (*a*) porcine and (*b*) ovine vitreous humor. The distribution curves contain data from > 1000 carboxyl-terminated (COOH), PEGylated (PEG) and amine-terminated (NH_2) 200 nm polystyrene particles. For the calculation of these distributions, data from at least three different vitreous samples have been pooled.

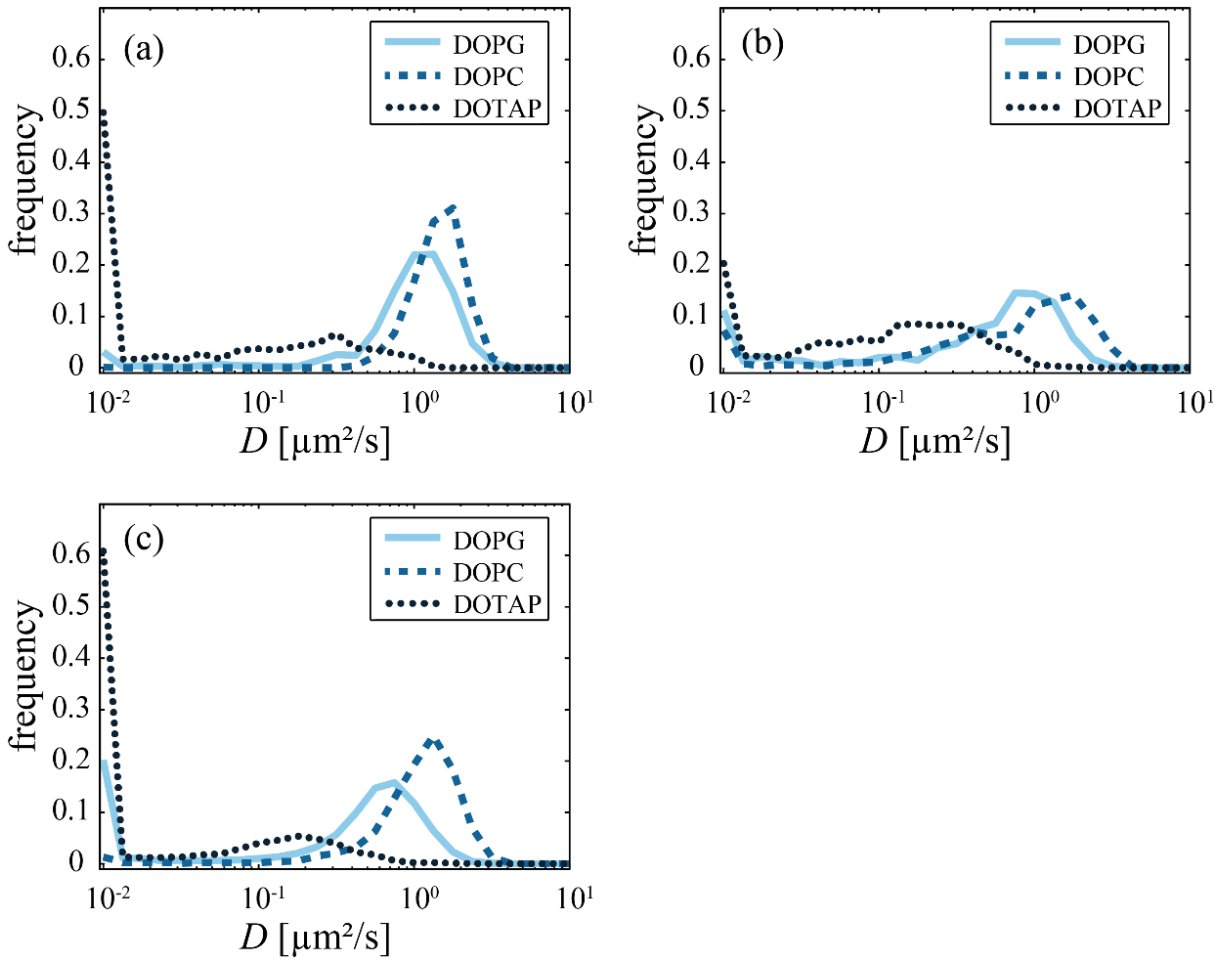

Fig. S2: Diffusive mobility of 200 nm liposomes in (*a*) bovine, (*b*) porcine and (*c*) ovine vitreous humor. The distribution curves contain data from > 1000 apparent diffusion coefficients is determined for DOPG, DOPC and DOTAP 200 nm liposomes in vitreous humor. For the calculation of these distributions, data from at least three different vitreous samples have been pooled.

Distribution of apparent diffusion coefficients for polystyrene particles in ovine vitreous humor at different injection volumes and different salt concentrations.

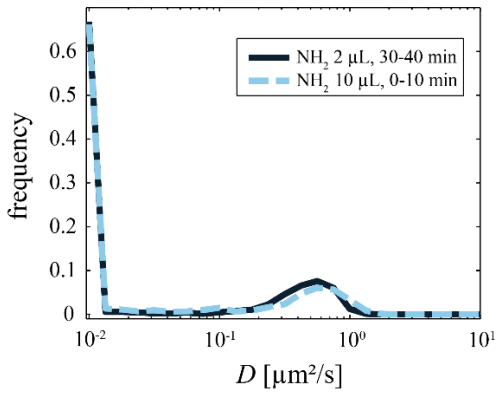

Fig. S3: Diffusive mobility of 200 nm polystyrene particles in ovine vitreous humor at different injection volumes and incubation times before SPT. Comparison of the diffusive mobility of amine-terminated polystyrene particles for injections of 10 µL particle solution into the vitreous (SPT was started 0-10 min after injection) and injection of 2 µL (SPT was started 30-40 min after injection). The distribution curves contain data from > 1000 apparent diffusion coefficients of amine-terminated (NH_2) 200 nm polystyrene particles. For the calculation of these distributions, data from at least three different vitreous samples have been pooled.

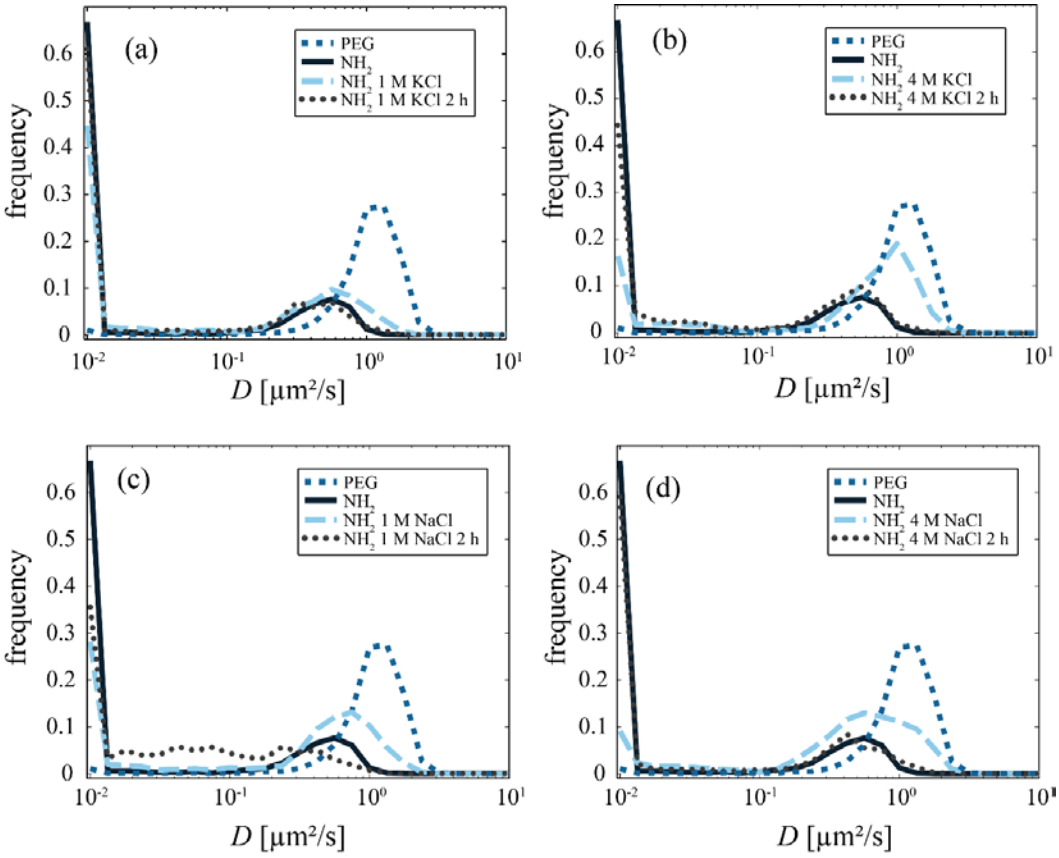

Fig. S4: Diffusive mobility of 200 nm polystyrene particles in ovine vitreous humor at various salt concentrations. Comparison of the diffusive mobility of amine-terminated polystyrene particles at different KCl (*a, b*) and NaCl (*c, d*) concentrations shortly after injection of a salt-particle solution and after 2 additional hours. PEGylated particles at physiological salt concentrations are shown as a reference for nearly free moving particles. The distribution curves contain data from > 1000 amine-terminated (NH_2) as well as PEGylated (PEG) 200 nm polystyrene particles. The peak of the mobile fraction of NH_2 particles is only increased in height but not shifted towards faster diffusion coefficients. Therefore, the NH_2 particles became more mobile but did not exhibit faster diffusion. For the calculation of these distributions, data from at least three different vitreous samples have been pooled.

Unconfined compression tests of ovine vitreous after incubation in high-salt solution

Compression experiments were performed on a rheometer (MCR 302, Anton Paar, Graz, Austria) using a plate-plate 25 mm measuring geometry (PP25, Anton Paar, Graz, Austria) with an indentation speed of 10 µm/s until a normal force of 0.5 N was reached. For measurements, the vitreous samples were placed in a 50 mm glass petri dish which was positioned in the middle of the measuring plate of the rheometer. Each vitreous humor sample was compressed three times to verify that the compression of the vitreous itself does not influence its mechanical integrity. Samples were compressed first in the fresh state and then again after a 5 h incubation in salt solution. The Young's moduli were calculated by fitting the stress/strain data for strains above 5 %.

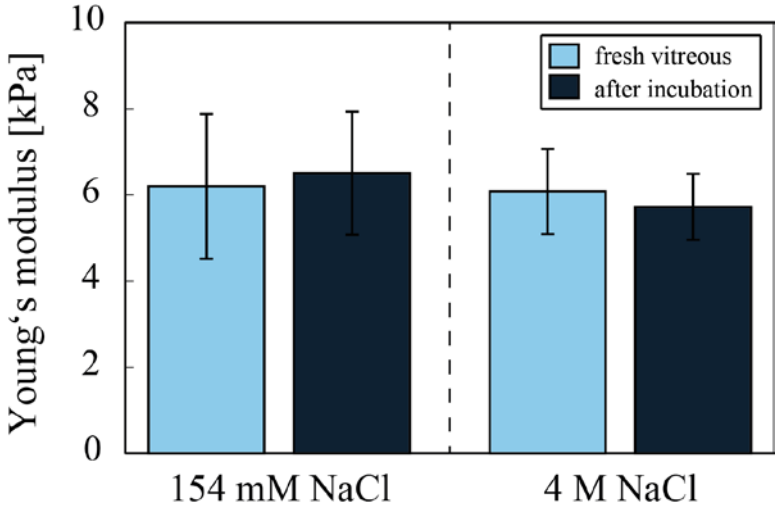

Fig. S5: Young's moduli of ovine vitreous humor after incubation in salt solutions. Unconfined compression tests were performed on ovine vitreous samples both in the fresh state and after those samples have been incubated for 5 hours either in a physiological (154 mM) NaCl solution or a high-salt (4 M) NaCl solution (pH 7). The error bars denote the standard deviation as obtained from three different vitreous samples.

Enzymatic removal of ovine vitreous humor components

Digestion of collagen II was performed by incubating fresh vitreous samples each in 7.5 mL 50 mM TRIS/HCl buffer (pH 7.4, 4 mM $CaCl_2$) containing 1 mg/mL of collagenase type II from *Clostridium histolyticum* at 37 °C overnight. Control samples were incubated at the same conditions but without the enzyme. Incubation of vitreous samples with collagenase type II resulted in total liquefaction of the vitreous (Fig. S6*a*) whereas the control samples maintained their structural integrity (Fig. S6*b*).

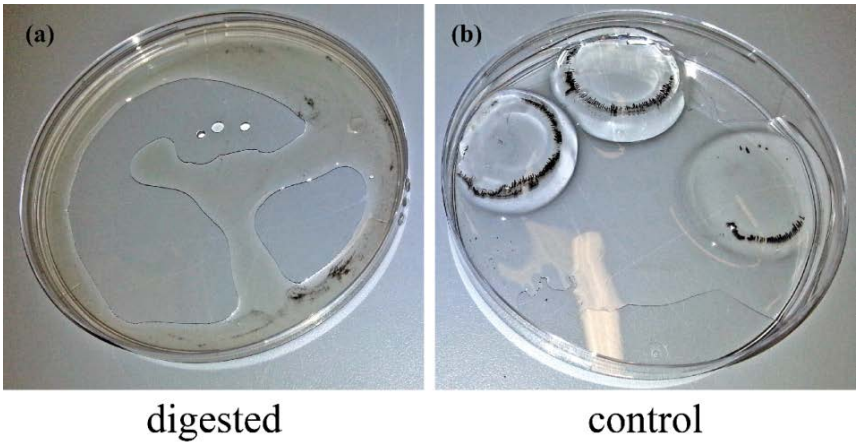

Fig. S6: Ovine vitreous humor after digestion with collagenase type II. Ovine vitreous humor samples are shown after 24 hour digestion with collagenase type II from *Clostridium histolyticum* (*a*). Control samples which were stored in digestion buffer but in the absence of enzymes are shown in (*b*).

Digestion of vitreous samples with heparinase and hyaluronidase was performed as described in the methods section of the main paper. Fig. S7 and S8 show that the treated vitreous samples maintained their structural integrity although the samples lost some water and slightly decreased in size as a consequence of the enzymatic treatment.

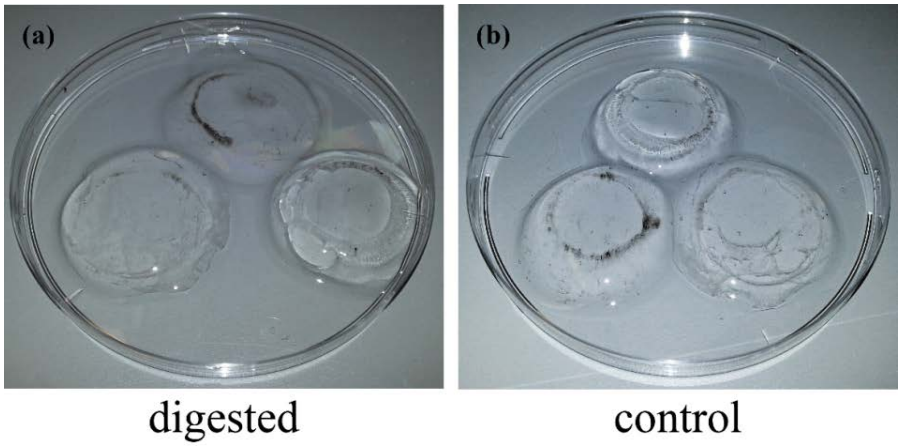

Fig. S7: Ovine vitreous humor after digestion with heparinase I and III. Ovine vitreous humor samples are shown after 72 hour digestion with heparinase I and III from *Flavobacterium heparinum* (*a*). Control samples which were stored in digestion buffer but in the absence of enzymes are shown in (*b*).

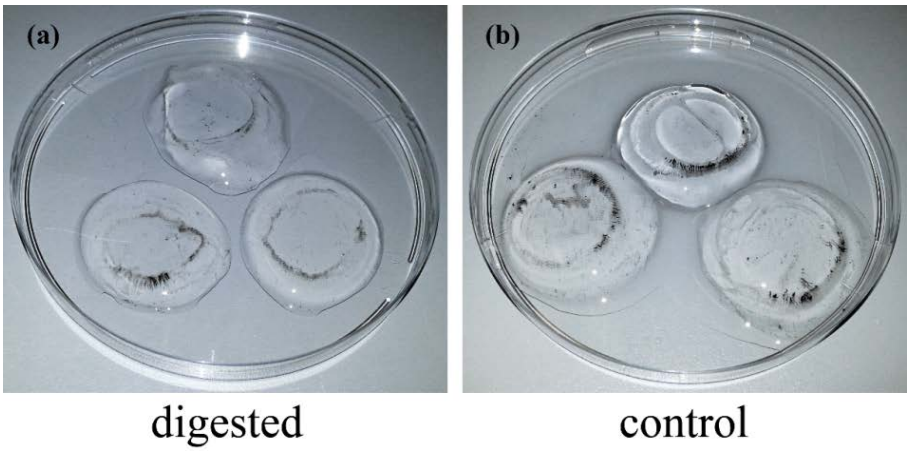

Fig. S8: Ovine vitreous humor after digestion with hyaluronidase. Ovine vitreous humor samples are shown after 72 hour digestion with hyaluronidase from *Streptomyces hyalurolyticus* (*a*). Control samples which were stored in digestion buffer but in the absence of enzymes are shown in (*b*).

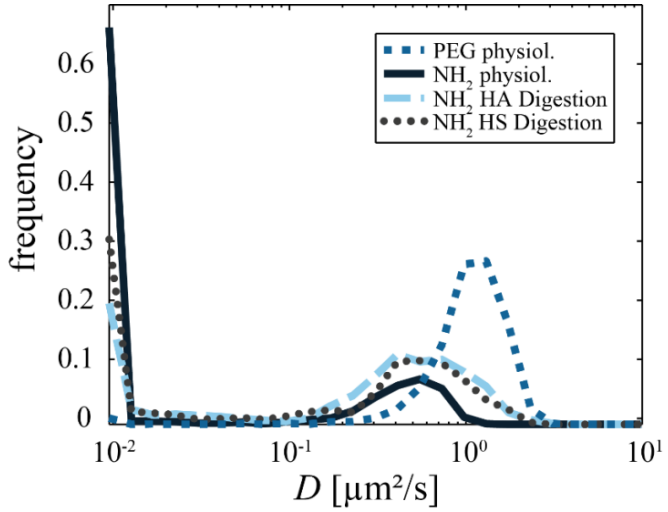

Fig. S9: Diffusive mobility of 200 nm polystyrene particles in ovine vitreous humor after digestion of HA or HS. Comparison of the diffusive mobility of amine-terminated polystyrene particles in vitreous humor at physiological conditions and after enzymatic removal of HA and HS. PEGylated particles at physiological salt concentrations are shown as a reference and represent nearly free moving particles. The distribution curves contain data from > 1000 apparent diffusion coefficients of amine-terminated (NH_2) 200 nm polystyrene particles. For the calculation of these distributions, data from at least three different vitreous samples have been pooled.

Table T2: Percentage of wet weight of ovine vitreous after enzymatic digestion of HA or HS. The percentage of wet weight was determined by weighing the vitreous samples before and after enzymatic treatment. The depicted percent values refer to the wet weight of fresh vitreous samples before the treatment (= 100 %). The errors denote the standard deviation as obtained from at least three vitreous samples.

wet weight compared to untreated state [%]	**control (buffer only)**	**digested**
treatment with hyaluronidase	80 ± 8.5	47 ± 7.2
treatment with heparinase	88 ± 3.5	75 ± 7.3

Penetration of molecules into ovine vitreous humor

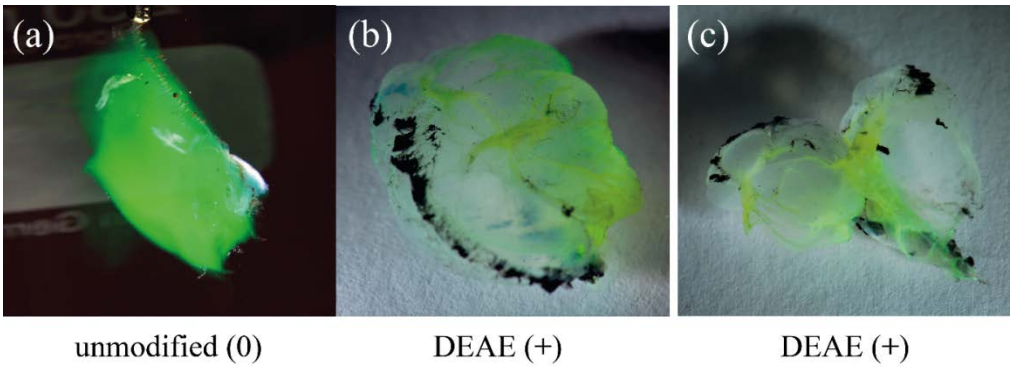

Fig. S10: Penetration of FITC-labeled 150 kDa dextrans into ovine vitreous humor. Ovine vitreous humor samples are shown after overnight incubation in unmodified (*a*) and cationic DEAE-modified (*b*, *c*) dextran solutions (dextran concentration in the incubation buffer was 10 mg/mL). Whereas the neutral dextrans are able to penetrate the whole vitreous humor (*a*), the cationic DEAE-dextrans accumulate at the outside of the vitreous (*b*) and are not able to penetrate into the bulk volume of the vitreous (*c*).

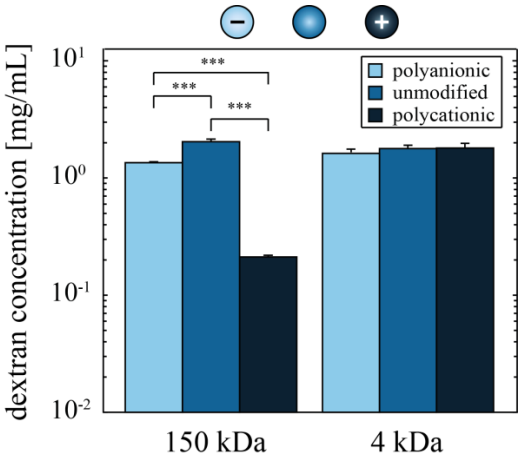

Fig S11: Penetration efficiency of different dextran molecules into ovine vitreous humor fragments. The concentration of dextrans in ovine vitreous humor is shown after incubation of the vitreous fragments overnight in different dextran solutions (dextran concentration in the incubation buffer was 10 mg/mL). DEAE (polycationic), unmodified (neutral) and CM (polyanionic) dextrans are compared at two different molecular weights. The error bars denote the standard deviation as obtained from three vitreous samples. Asterisks denote statistically significant differences (*** *:=* $p < 0.001$).

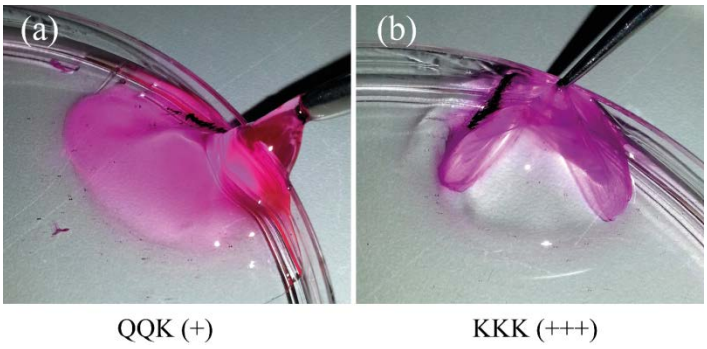

Fig. S12: Penetration of TAMRA-labeled oligopeptides into ovine vitreous humor. Ovine vitreous humor samples are shown after overnight incubation in $(QQK)_8$ (*a*) and $(KKK)_8$ (*b*) peptide solutions prepared at 1 mg/ml. Whereas the slightly positive oligopeptide $(QQK)_8$ is able to penetrate the whole vitreous humor (*a*), the strongly cationic $(KKK)_8$ accumulates at the outside of the vitreous (*b*) and is not able to penetrate the bulk volume of the vitreous.